Outflow Tract Ablation Using a Conditionally Cytotoxic Feline Immunodeficiency Viral Vector

Ze Zhang,[1] Amardeep S. Dhaliwal,[2] Harry Tseng,[3] James D. Kim,[2] Joel S. Schuman,[2,4] Robert N. Weinreb,[5] and Nils A. Loewen[2]

[1]Yale University School of Medicine, New Haven, Connecticut
[2]University of Pittsburgh Medical Center Eye Center, Ophthalmology and Visual Science Research Center, Department of Ophthalmology, University of Pittsburgh School of Medicine, Pittsburgh, Pennsylvania
[3]Albany Medical College, Albany, New York
[4]Department of Bioengineering, Swanson School of Engineering, University of Pittsburgh, Pittsburgh, Pennsylvania
[5]Department of Ophthalmology and Hamilton Glaucoma Center, University of California-San Diego, San Diego, California

Correspondence: Nils A. Loewen, 203 Lothrop Street, #819, Pittsburgh, PA
loewen.nils@gmail.com.

Submitted: July 22, 2013
Accepted: January 2, 2014

Citation: Zhang Z, Dhaliwal AS, Tseng H, et al. Outflow tract ablation using a conditionally cytotoxic feline immunodeficiency viral vector. *Invest Ophthalmol Vis Sci*. 2014;55:935–940. DOI:10.1167/iovs.13-12890

Purpose. To create an in vivo model of vector-mediated trabecular meshwork (TM) ablation and replacement.

Methods. We generated a conditionally cytotoxic, trackable vector, HSVtkiG, that expressed herpes simplex virus 1 thymidine kinase (HSVtk) and enhanced green fluorescent protein (eGFP). We optimized HSVtkiG ablation in vitro with ganciclovir (GCV) in comparison to eGFP control vector GINSIN and investigated the mechanism. Right eyes of 24 rats were then injected intracamerally with either HSVtkiG or GINSIN, before intraperitoneal GCV was administered 1 week later. Intraocular pressure, central corneal thickness (CCT), and slit-lamp exams were assessed for 8 weeks. Transduction and ablation were followed by gonioscopic visualization of eGFP. Histology was obtained with TM cell counts and immunohistochemistry markers of inflammation.

Results. Transduction and ablation parameters were established in vitro. Apoptosis was the cause of cell death. In vivo, transduction was seen gonioscopically to be targeted to the TM, followed by disappearance of eGFP marker fluorescence in HSVtkiG-transduced cells after injection of GCV. Ablation resulted in an IOP decrease of 25% in HSVtkiG-injected eyes 2 days after GCV but not in GINSIN or noninjected control eyes ($P < 0.05$). Trabecular meshwork cellularity was decreased at the time of lowest IOP and recovered thereafter, while CCT remained unchanged. Inflammation was absent.

Conclusions. A vector-based system for inducible ablation of cells of the outflow tract was developed. Trabecular meshwork ablation lowered IOP, and recovery of cellularity and IOP followed. This model may be useful to study pressure regulation by the TM, its stem cells, and migration patterns.

Keywords: glaucoma, trabecular meshwork, gene therapy, ablation

Primary open angle glaucoma (POAG) is characterized by decreased outflow through the trabecular meshwork (TM) that results in elevated intraocular pressure (IOP) and progressive damage of the optic nerve.[1,2] Conflicting theories exist regarding whether outflow resistance is primarily the result of decreasing cell count and function of the TM[3,4] and Schlemm's canal (SC)[5] or accumulation of extracellular matrix in the TM,[6–8] or a combination of both. Evidence has emerged that TM stem cells may be directly anterior to or distributed within the substance of the TM and can be activated after injury or dormant in the TM itself.[9–11] The declining turnover of TM cells in glaucoma is poorly understood because practical tools do not exist to selectively ablate these cells to study cell division and migration.

We hypothesize that failure of outflow regulation can be corrected using strategies of reverse engineering by ablating and rebuilding this structure. Recreating a normal, regulating barrier rather than simply removing[12] or bypassing it[13] has clinical relevance by keeping the aqueous humor separate from the protein- and cell-rich intravascular space[14] and avoids complications that are typical for IOP-reducing devices and antimetabolite-enhanced filtering procedures.[15] This approach may also provide tools to study fundamental questions of cell migration and progenitor cell locations.

Methods

Feline Immunodeficiency Viral Vector Construction

Vesicular stomatitis virus glycoprotein G-pseudotyped (VSV-G) feline immunodeficiency viral (FIV) vectors were produced as previously described, using a tripartite vector system consisting of envelope plasmid pMD.G, packaging plasmid pFP93, and two different FIV transfer vectors, pHSVtkiG and pGINSIN (Fig. 1).[16,17] Control vector GINSIN encoded enhanced green fluorescent protein (eGFP), and neomycin resistance via an

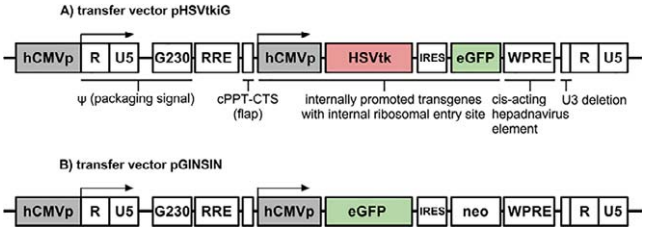

Figure 1. Map of FIV vectors. (**A**) eGFP-expressing transfer vector pHSVtkiG. (**B**) eGFP-expressing transfer vector pGINSIN. hCMVp, CMV promoter; RRE, Rev-response element; neo, neomycin resistance; WPRE, woodchuck hepatitis posttranscriptional regulatory element; cPPT, central polypurine tract; CTS, central termination sequence.

internal ribosomal entry site (IRES). Vector HSVtkiG expressed herpes simplex virus 1 thymidine kinase (HSVtk) (No. 12382; Addgene, Cambridge, MA) via a cytomegalovirus (CMV) promoter and eGFP via an IRES. Herpes simplex virus 1 thymidine kinase converts nucleotide analogues to the diphosphorylated form, which can be converted by cellular tyrosine kinases to the toxic triphosphate form that competes with normal nucleosides in DNA replication, preventing elongation due to base pair mismatches, DNA breakage, and fragmentation.[18] Feline immunodeficiency viral vectors were produced by transient transfection and ultracentrifugation, and titrated by fluorescence-assisted flow cytometry (FACS) analysis.[19]

In Vitro Studies

NTM5 cells (gift from Alcon, Fort Worth, TX) and CrFK cells (CCL-94; American Type Culture Collection, Manassas, VA) were transduced with escalating multiplicities of infection (MOIs of 3, 5, 10, and 30) of either GINSIN or HSVtkiG vector. NTM5 cells were also growth arrested with aphidicolin (15 μg/mL; Sigma-A0781; Sigma-Aldrich, St. Louis, MO) for 24 hours prior to administration of ganciclovir (GCV) and for the remainder to simulate TM in situ conditions more realistically and to test whether GCV toxicity on DNA replication[18] was present in the absence of cell division. Aphidicolin was maintained in all media overlying growth-arrested cells throughout the experiment and was replenished daily. Cells transduced with an MOI of 5 were expanded for ablation using 30 mg/mL GCV (AK Scientific, Union City, CA). When nuclei of HSVtkiG-transduced, GCV-exposed cells became pyknotic and cells started to detach at 24 hours, a terminal deoxynucleotidyl transferase dUTP nick-end labeling (TUNEL) assay (Click-iT TUNEL Alexa Fluor 594 Imaging Assay; Life Technologies, Carlsbad, CA), a method for detecting DNA fragmentation by labeling the terminal end of nucleic acids, was deployed to confirm apoptosis as the mechanism of cell death (Figs. 2J, 2K). Nuclei were counterstained with Hoechst 33342 (Life Technologies). Consistent with the timing of apoptosis, cell death could be seen unaided starting at 24 hours and was complete by 48 hours when lysis caused disappearance of fluorescence. Images were captured using a digital camera (Coolpix 900; Nikon, Melville, NY) mounted on a fluorescence-capable, inverted microscope with an eGFP-optimized filter cube (Axiovert; Zeiss, Oberkochen, Germany) at 24 and 48 hours after GCV exposure.

In Vivo Studies

All animals were handled in accordance with the ARVO Statement for the Use of Animals in Ophthalmic and Vision Research, and all protocols were approved and monitored by the Yale University Institutional Animal Care and Use

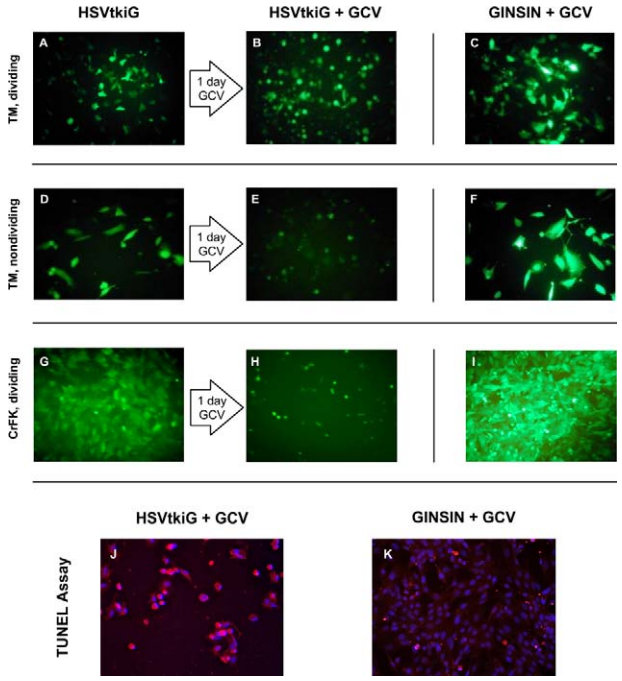

Figure 2. Conditional ganciclovir-mediated cytotoxicity of vector HSVtkiG. *Top row*: HSVtkiG-transduced NTM5 TM cells (**A**) detach within 1 day of GCV exposure (**B**) before lysis. *Right column*: Control vector GINSIN-transduced cells are not affected by GCV (**C**, **F**, **I**). *Second row*: NTM5 cells (**D**) were growth arrested with aphidicolin to mimic in situ conditions. Detachment and lysis occurs within 1 day (**E**). *Third row*: HSVtkiG-transduced CrFK cells (**G**) detach and lyse (**H**). *Bottom row*: HSVtkiG-transduced cells enter apoptosis within 24 hours after GCV ([**J**] *red* cell bodies, pyknotic *blue* nuclei) but not GINSIN-transduced cells (**K**).

Committee. Eight-week-old female Sprague-Dawley rats (Charles River, Wilmington, MA) were allowed to acclimate for 3 days before daily IOP and central corneal thickness (CCT) measurements were performed for 7 consecutive days as well as on days 1, 3, 7, 10, and 14, and then weekly.

Examination and Measurements

Anterior segments of live animals were examined by high-power and fluorescent microscopy and by direct gonioscopy. Briefly, animals were anesthetized with intraperitoneal ketamine (#00409205310, 65 mg/kg; Hospira, Inc., Lake Forest, IL) and xylazine (#4821, 5 mg/kg; Lloyd, Inc., Shenandoah, IA); viscoelastic was applied to the eye before the animal was placed on a slide facing the objective of the inverted microscope. Intraocular pressure was measured in restrained animals with a rebound tonometer (iCare, Espoo, Finland) at the same time of day, taken in triplicate, and reported as the mean. As an indirect test for endothelial function and IOP confounder, pachymetric CCT (DGH Technology, Exton, PA) was measured after topical anesthesia (0.5% proparacaine; Alcon), obtained in triplicate, and reported as the mean.

In Vivo Transduction

All procedures were performed in anesthetized animals as described above but using sterile techniques and an animal surgery suite with a motorized ophthalmic surgery microscope (Carl Zeiss Meditec AG, Jena, Germany).

On day 0, 5 μL aqueous humor was withdrawn from anterior chambers with a 30-gauge subcutaneous needle. A

vector bolus of 5 μL with 1.5 × 10E9 TU/mL FIV was then injected intracamerally with a custom-made 32-gauge needle (30° bevel, 9.52-mm-long needle, 10-μL microsyringe [Hamilton, Reno, NV]). The needle was left in place in the well-pressurized eye for 30 seconds to prevent reflux of injected vector. Injected eyes received a drop of 1% prednisolone acetate (Alcon) and 0.5% moxifloxacin (Alcon). On day 7, GCV was administered intraperitoneally for 4 consecutive days at 25 mg/kg twice a day.

Histology

After animals were euthanized (1 mL intraperitoneal Euthasol; Virbac Corp., Fort Worth, TX), enucleated eyes were fixated in 10% buffered formalin for 24 hours before paraffin embedding to generate 5-μm hematoxylin and eosin sections. For TM cell counts, slides were randomly selected in blinded fashion with equal numbers of two eyes until 10 TM sections had been counted per group. Whenever possible, both opposing TM sections per slide were assessed in these whole eye preparations. An unpaired Student's *t*-test was used for statistical analysis to compare HSVtk, GINSIN, and control eyes.

Seven days after transduction when cellularity changes in the TM were the most notable, additional sections were obtained from HSVtkiG- and GINSIN-transduced eyes and normal contralateral control eyes and examined by immunohistochemistry using anti-GFP, anti-CD3, and antimacrophage antibodies. These tissue sections were first deparaffinized, rehydrated through stepped ethanol–water baths, and placed for 30 minutes into a steamer with citrate buffer to maximize antigen retrieval. Slides were incubated overnight with anti-GFP (ab13970, 1:300 dilution; AbCam, Cambridge, UK), anti-CD3 (ab5690, 1:50; AbCam), antimacrophage (ab134795, 1:100; AbCam), followed by secondary antibody staining using a peroxidase-based and aminoethylcarbazole (AEC) chromogenic substrate. Sections were counterstained with 4′,6-diamidino-2-phenylindole for nuclei. Positive controls consisted of eGFP transgenic zebrafish and spleen as recommended by the manufacturers and were processed using the same protocol in the same session.

Statistical Analysis

Our power calculation showed that we needed $n = 12$ animals to have 80% power to detect an IOP difference of 3 mm Hg with a standard deviation of 1.5 mm Hg using a paired *t*-test and an alpha error of 0.05. All IOP and CCT data were entered using Excel 2010 (Microsoft, Redmond, WA) and transferred to SPSS for analysis (version 20; Chicago, IL). Student's *t*-test was performed to compare IOP and CCT between groups. Differences were considered statistically significant if $P < 0.05$. Statistical significance between groups was determined with statistical analysis software (SPSS version 20).

Results

In Vitro Vector Function

Internal ribosomal entry site–mediated eGFP expression of HSVtkiG-transduced cells was relatively less fluorescent than cap-dependent, CMV promoter-driven eGFP expression in GINSIN-transduced cells (Fig. 2). HSVtkiG at an MOI of 5 and 30 μg/mL GCV caused the fastest detachment and death of transduced NTM5 and CrFK cells, resulting in lysis within 48 hours of exposure, while control cells transduced with HSVtkiG without GCV, as well as GINSIN with and without GCV, were unaffected, growing to full confluence in the same time (Fig. 2).

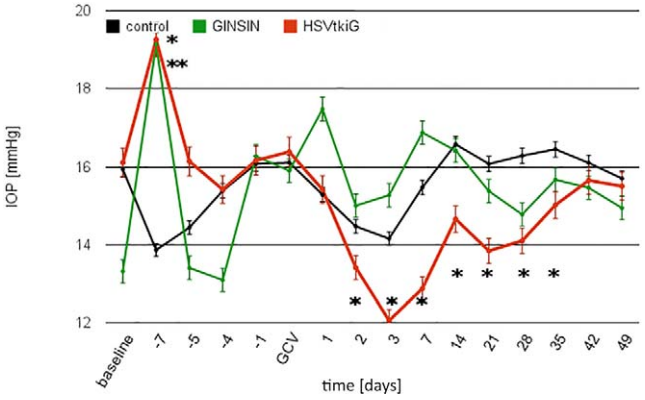

Figure 3. Intraocular pressure over time. IOP increased in both GINSIN and HSVtkiG compared to controls (day −7, *HSVtkiG, **GINSIN, $P < 0.05$) but returned to baseline within 1 day. After GCV administration, IOP decreased significantly in HSVtkiG only, with the decrease persisting through day 35 ($n = 12$ per group).

In Vivo TM Transduction and Ablation

Transduction with both HSVtkiG and GINSIN increased IOP significantly compared to that in noninjected control eyes for the first 24 hours before it returned to baseline the next day (Fig. 3, $P < 0.05$). When GCV was administered intraperitoneally 1 week after transduction, IOP started to decrease significantly on day 2, reaching a trough of 25% reduction at day 3 ($n = 10$, $P < 0.05$, Fig. 3), but not in noninjected control eyes or GINSIN eyes. This difference persisted, slowly approaching baseline by day 42. There was no ciliary flush, and on high-power microscopy no increased flare or anterior chamber cells were observed at any time following transduction.

The baseline CCT of 174 ± 2 μm was briefly increased for 24 (GINSIN) or 76 hours (HSVtkiG), respectively, following injection of vectors compared to noninjected control eyes, but there was no difference between control and transduced eyes for the remainder of the study ($P < 0.05$).

Expression of eGFP from both GINSIN and HSVtkiG was limited to the TM (Fig. 4), with only occasional eGFP-positive corneal endothelial cells. Fluorescence could be visualized gonioscopically from day 7 onward after transduction (Fig. 4) and disappeared 3 days after intraperitoneal GCV in the HSVtkiG eyes. In contrast, expression persisted for the remainder of the experiments in GINSIN and additional nonablated HSVtkiG eyes.

Similar to what was seen in our initial in vitro experiments, TM cells of HSVtkiG eyes rounded up and appeared to be

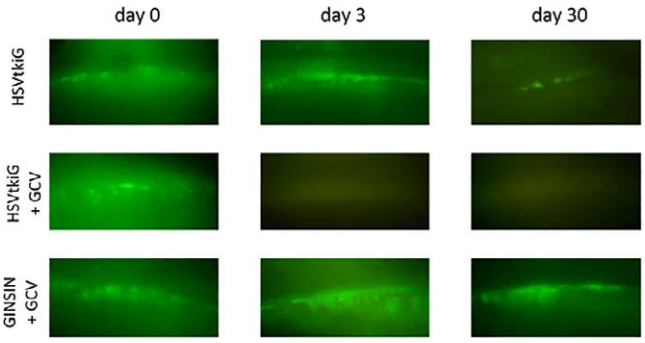

Figure 4. Direct gonioscopy of rat TM. HSVtkiG-transduced eyes lost eGFP marker expression after GCV administration. Fluorescence persisted in HSVtkiG control eyes not exposed to GCV and GINSIN eyes of GCV-exposed animals.

Investigative Ophthalmology & Visual Science

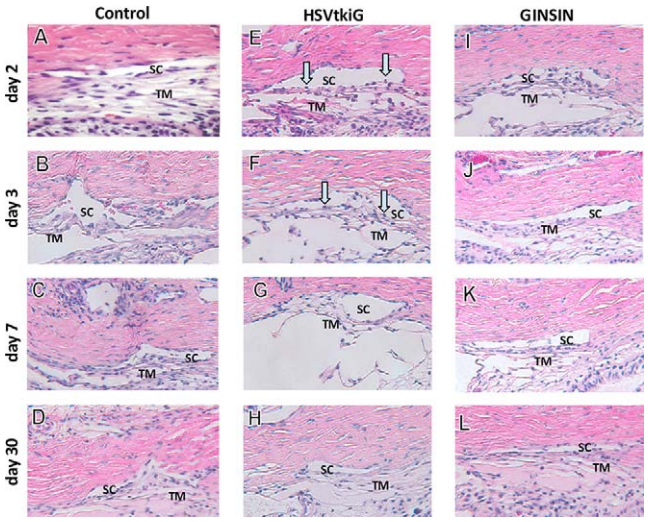

Figure 5. Histology of TM and SC. On day 2 (**E**) and day 3 (**F**) after GCV, TM cells of HSVtkiG-transduced eyes rounded up and detached (*blue arrows*), similarly to what occurred in in vitro experiments. Trabecular meshwork of HSVtkiG eyes then recovered slowly (**G**, **H**). GINSIN-transduced eyes did not experience a loss of TM cells following exposure to GCV (**I–L**) when compared to control eyes (**A–D**).

detaching on day 2 after GCV administration, followed by decreased cellularity that slowly recovered (Fig. 5). Control eyes remained unchanged. There was no other difference in anterior or posterior segment appearance of GINSIN, HSVtkiG, and control eyes.

Immunohistochemistry did not detect macrophages or T-cells in transduced eyes or normal control eyes, while positive controls showed high levels of the antigens tested for.

Cell counts indicated a significant reduction of TM cells in HSVtkiG-transduced eyes on day 2 that subsequently increased (Fig. 6).

Discussion

In this study we attempted to develop an in vitro and in vivo model of TM ablation to provide new tools to study migration and regeneration in the outflow tract. The declining turnover of TM cells in glaucoma is poorly understood. Evidence has emerged that neural crest progenitors may exist directly anterior to the TM at the insert zone and may be activated after injury.[9,10] Recent reports suggest that stem cell–based approaches might be feasible.[11,20]

Although lentiviral vectors are typically used to achieve stable long-term expression in nondividing cells, we took advantage of their ability to transduce TM preferentially[17] and to coexpress a trackable marker.[21] We selected the rat because rats are small in size and have been previously used to study outflow.[22–24] The HSVtk ablation strategy deployed here by inducing apoptosis using GCV has been used extensively in cancer gene therapy to lyse tumors while limiting the bystander effect on nontransduced tissue.[18,25]

After establishing vector function in vitro, we found that the TM could be targeted with a small intracameral vector bolus and followed in vivo. Similar to our studies in cat, monkey, and human eyes,[17,21,26,27] there was no apparent toxicity to adjacent structures on high-power biomicroscopy, gonioscopy, and histology. Although HSVtk-mediated ablation can have a bystander effect on nontransduced, adjacent cells via gap junctions,[28–31] this effect may be limited here due to efficient washout directly through this structure. The temporary CCT increase immediately following vector injection matched trauma from needle insertion and was quickly reversible. In contrast, induction of TM cell ablation in HSVtkiG-transduced eyes did not have a notable effect on CCT or corneal histology, consistent with marker gene expression that was limited to this structure.

Although rat TM may be less able than human TM to generate a high flow resistance because it is only a few cell layers thick, we did see a decrease of IOP that became observable within 24 hours after GCV-mediated induction of ablation, reaching 25% reduction on day 3. There was no ciliary flush, and on high-power microscopy no flare or anterior chamber cells suggesting an iritis were observed. We further investigated the changes in cellularity that coincided with the IOP response to test for a T-cell– or macrophage-mediated immune response but could not detect these cell types. Feline immunodeficiency viral vectors expressing marker genes in other in vivo studies left IOP largely unaffected, and no inflammation was seen.[21,32] The IOP drop seen in this study correlated well with the temporal pattern of our in vitro experiments and the gonioscopically disappearing eGFP fluorescence on day 2 and histology. Intraocular pressure reduction took 5 weeks to increase to preablation levels. The decreased cellularity and extended IOP reduction seen here were different from what is observed with agents that relax the TM by acting on the cytoskeleton,[33–35] and more akin to TM

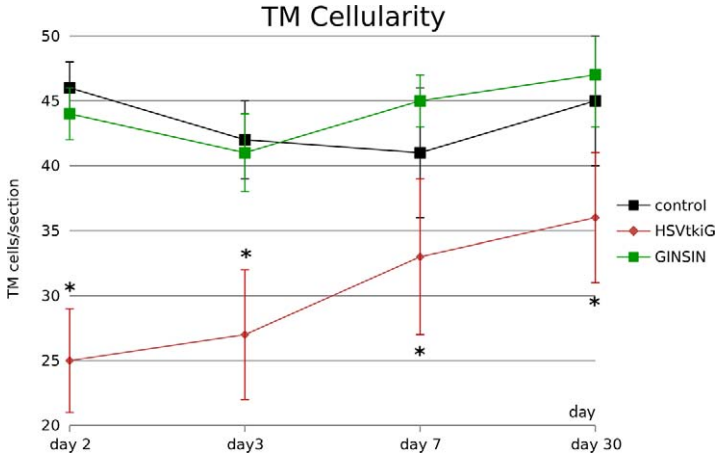

Figure 6. Trabecular meshwork cellularity. Following GCV-mediated ablation, HSVtkiG-transduced eyes had significantly fewer cells than control or GINSIN eyes, but the number increased subsequently (*$P < 0.05$, 10 sections from two eyes per data point).

Investigative Ophthalmology & Visual Science

cell loss as can be seen with ethacrynic acid[36] when the cellular outflow barrier that the TM presents is eliminated.[37]

More subtle changes may have also contributed to the observed effect. Decreased IOP for several days after transduction with both the control vector, GINSIN, and the cytoablative vector, HSVtkiG, could be the result of activation of a stress response pathway as seen after trabeculoplasty,[38] phacoemulsification,[39] or chronic dysfunction in glaucoma,[40] and sublethally ablated TM cells in HSVtkiG eyes may have experienced additional enhancement.

Our study was designed to be properly powered to detect an IOP change, and it was challenging to capture and quantify the rapidly unfolding morphological cell changes because rat TM has only a few cell layers compared to that in primate eyes.[21,32] Our findings indicate that healthy TM cells are vital to regulate pressure with an outflow resistance in the rat of at least 25% in this structure. Trabecular meshwork cell ablation, even if incomplete, results in IOP reduction. It would be interesting to investigate TM ablation strategies in new glaucoma models, in particular whether such a cell-based approach will work in a rat model with TM-specific, bone morphogenetic protein 2 (BMP2)-mediated IOP elevation that experiences TM calcification and accumulation of extracellular matrix that may more closely reflect human glaucoma.[41]

In conclusion, we demonstrated ablation of TM cells in vitro and in vivo using a conditionally cytotoxic FIV vector resulting in significant decrease in IOP and no damage to surrounding structures. This model may enable future studies of migration and regeneration of TM cells and their progenitors that are incompletely understood.

Acknowledgments

Supported in part by an unrestricted grant from Research to Prevent Blindness (New York, New York) (RNW), a Clinician Scientist grant from the American Glaucoma Society (NAL), an unrestricted grant from Research to Prevent Blindness (New York, New York) (JSS), The Eye & Ear Foundation of Pittsburgh (JSS), and National Institutes of Health Grant K08EY022737-01 (NAL).

Disclosure: **Z. Zhang**, None; **A.S. Dhaliwal**, None; **H. Tseng**, None; **J.D. Kim**, None; **J.S. Schuman**, None; **R.N. Weinreb**, None; **N.A. Loewen**, None

References

1. Larsson LI, Rettig ES, Brubaker RF. Aqueous flow in open-angle glaucoma. *Arch Ophthalmol*. 1995;113:283–286.
2. Toris CB, et al. Aqueous humor dynamics in ocular hypertensive patients. *J Glaucoma*. 2002;11:253–258.
3. Alvarado J, Murphy C, Juster R. Trabecular meshwork cellularity in primary open-angle glaucoma and nonglaucomatous normals. *Ophthalmology*. 1984;91:564–579.
4. Alvarado J, et al. Age-related changes in trabecular meshwork cellularity. *Invest Ophthalmol Vis Sci*. 1981;21:714–727.
5. Ainsworth JR, Lee WR. Effects of age and rapid high-pressure fixation on the morphology of Schlemm's canal. *Invest Ophthalmol Vis Sci*. 1990;31:745–750.
6. Lutjen-Drecoll E, Futa R, Rohen JW. Ultrahistochemical studies on tangential sections of the trabecular meshwork in normal and glaucomatous eyes. *Invest Ophthalmol Vis Sci*. 1981;21:563–573.
7. Alvarado JA, Yun AJ, Murphy CG. Juxtacanalicular tissue in primary open angle glaucoma and in nonglaucomatous normals. *Arch Ophthalmol*. 1986;104:1517–1528.
8. Stone EM, et al. Identification of a gene that causes primary open angle glaucoma. *Science*. 1997;275:668–670.
9. Raviola G. Schwalbe line's cells: a new cell type in the trabecular meshwork of Macaca mulatta. *Invest Ophthalmol Vis Sci*. 1982;22:45–56.
10. Gonzalez P, et al. Characterization of free-floating spheres from human trabecular meshwork (HTM) cell culture in vitro. *Exp Eye Res*. 2006;82:959–967.
11. Du Y, et al. Multipotent stem cells from trabecular meshwork become phagocytic TM cells. *Invest Ophthalmol Vis Sci*. 2012;53:1566–1575.
12. Francis BA, et al. Ab interno trabeculectomy: development of a novel device (Trabectome) and surgery for open-angle glaucoma. *J Glaucoma*. 2006;15:68–73.
13. Gedde SJ, et al. Treatment outcomes in the Tube Versus Trabeculectomy (TVT) study after five years of follow-up. *Am J Ophthalmol*. 2012;153:789–803, e2.
14. Jampel HD. Determination of protein concentration in aqueous humor. *J Glaucoma*. 1994;3:5–11.
15. Gedde SJ, et al. Surgical complications in the Tube Versus Trabeculectomy Study during the first year of follow-up. *Am J Ophthalmol*. 2007;143:23–31.
16. Loewen N, et al. FIV vectors. *Methods Mol Biol*. 2003;229:251–271.
17. Loewen N, et al. Preservation of aqueous outflow facility after second-generation FIV vector-mediated expression of marker genes in anterior segments of human eyes. *Invest Ophthalmol Vis Sci*. 2002;43:3686–3690.
18. Kaina B. DNA damage-triggered apoptosis: critical role of DNA repair, double-strand breaks, cell proliferation and signaling. *Biochem Pharmacol*. 2003;66:1547–1554.
19. Saenz DT, et al. Titration of feline immunodeficiency virus-based lentiviral vector preparations. *Cold Spring Harb Protoc*. 2012;1:126–128.
20. Du Y, et al. Stem cells from trabecular meshwork home to TM tissue in vivo. *Invest Ophthalmol Vis Sci*. 2013;54:1450–1459.
21. Loewen N, et al. Long-term, targeted genetic modification of the aqueous humor outflow tract coupled with noninvasive imaging of gene expression in vivo. *Invest Ophthalmol Vis Sci*. 2004;45:3091–3098.
22. Kee C, Sohn S, Hwang JM. Stromelysin gene transfer into cultured human trabecular cells and rat trabecular meshwork in vivo. *Invest Ophthalmol Vis Sci*. 2001;42:2856–2860.
23. Budenz DL, et al. In vivo gene transfer into murine corneal endothelial and trabecular meshwork cells. *Invest Ophthalmol Vis Sci*. 1995;36:2211–2215.
24. Buie LK, et al. Self-complementary AAV virus (scAAV) safe and long-term gene transfer in the trabecular meshwork of living rats and monkeys. *Invest Ophthalmol Vis Sci*. 2010;51:236–248.
25. Thust R, et al. Comparison of the genotoxic and apoptosis-inducing properties of ganciclovir and penciclovir in Chinese hamster ovary cells transfected with the thymidine kinase gene of herpes simplex virus-1: implications for gene therapeutic approaches. *Cancer Gene Ther*. 2000;7:107–117.
26. Loewen N, et al. Genetic modification of human trabecular meshwork with lentiviral vectors. *Hum Gene Ther*. 2001;12:2109–2119.
27. Khare PD, et al. Durable, safe, multi-gene lentiviral vector expression in feline trabecular meshwork. *Mol Ther*. 2008;16:97–106.
28. Pu K, et al. Bystander effect in suicide gene therapy using immortalized neural stem cells transduced with herpes simplex virus thymidine kinase gene on medulloblastoma regression. *Brain Res*. 2011;1369:245–252.
29. Dachs GU, et al. Bystander or no bystander for gene directed enzyme prodrug therapy. *Molecules*. 2009;14:4517–4545.

30. Nicholas TW, et al. Suicide gene therapy with herpes simplex virus thymidine kinase and ganciclovir is enhanced with connexins to improve gap junctions and bystander effects. *Histol Histopathol*. 2003;18:495–507.
31. Namba H, et al. Efficacy of the bystander effect in the herpes simplex virus thymidine kinase-mediated gene therapy is influenced by the expression of connexin43 in the target cells. *Cancer Gene Ther*. 2001;8:414–420.
32. Barraza RA, et al. Prolonged transgene expression with lentiviral vectors in the aqueous humor outflow pathway of nonhuman primates. *Hum Gene Ther*. 2009;20:191–200.
33. Sabanay I, et al. H-7 effects on the structure and fluid conductance of monkey trabecular meshwork. *Arch Ophthalmol*. 2000;118:955–962.
34. O'Brien ET, et al. A mechanism for trabecular meshwork cell retraction: ethacrynic acid initiates the dephosphorylation of focal adhesion proteins. *Exp Eye Res*. 1997;65:471–483.
35. Sabanay I, et al. Latrunculin B effects on trabecular meshwork and corneal endothelial morphology in monkeys. *Exp Eye Res*. 2006;82:236–246.
36. Liang LL, et al. Ethacrynic acid increases facility of outflow in the human eye in vitro. *Arch Ophthalmol*. 1992;110:106–109.
37. Maepea O, Bill A. Pressures in the juxtacanalicular tissue and Schlemm's canal in monkeys. *Exp Eye Res*. 1992;54:879–883.
38. Alvarado JA, et al. A new insight into the cellular regulation of aqueous outflow: how trabecular meshwork endothelial cells drive a mechanism that regulates the permeability of Schlemm's canal endothelial cells. *Br J Ophthalmol*. 2005; 89:1500–1505.
39. Wang N, et al. Ultrasound activates the TM ELAM-1/IL-1/NF-kappaB response: a potential mechanism for intraocular pressure reduction after phacoemulsification. *Invest Ophthalmol Vis Sci*. 2003;44:1977–1981.
40. Wang N, et al. Activation of a tissue-specific stress response in the aqueous outflow pathway of the eye defines the glaucoma disease phenotype. *Nat Med*. 2001;7:304–309.
41. Buie LK, et al. Development of a model of elevated intraocular pressure in rats by gene transfer of bone morphogenetic protein 2 (BMP2). *Invest Ophthalmol Vis Sci*. 2013;54:5441–5455.

Investigative Ophthalmology & Visual Science